Applied Microbiology and Biotechnology (2022) 106:2091–2106
https://doi.org/10.1007/s00253-022-11830-4

GENOMICS, TRANSCRIPTOMICS, PROTEOMICS

Transcriptomics analyses and biochemical characterization of *Aspergillus flavus* spores exposed to 1-nonanol

Yu-Liang Qin[1,2] · Shuai-Bing Zhang[1,2] · Yang-Yong Lv[1,2] · Huan-Chen Zhai[1,2] · Yuan-Sen Hu[1,2] · Jing-Ping Cai[1,2]

Received: 29 December 2021 / Revised: 28 January 2022 / Accepted: 5 February 2022 / Published online: 18 February 2022

Abstract

The exploitation of plant volatile organic compounds as biofumigants to control postharvest decaying of agro-products has received considerable research attention. Our previous study reported that 1-nonanol, the main constituent of cereal volatiles, can inhibit *Aspergillus flavus* growth and has the potential as a biofumigant to control the fungal spoilage of cereal grains. However, the antifungal mechanism of 1-nonanol against *A. flavus* is still unclear at the molecular level. In this study, the minimum inhibitory concentration and minimum fungicidal concentration of 1-nonanol against *A. flavus* spores were 2 and 4 μL/mL, respectively. Scanning electron microscopy revealed that the 1-nonanol can distort the morphology of *A. flavus* spore. Annexin V-FITC/PI double staining showed that 1-nonanol induced phosphatidylserine eversion and increased membrane permeability of *A. flavus* spores. Transcriptional profile analysis showed that 1-nonanol treatment mainly affected the expression of genes related to membrane damage, oxidative phosphorylation, blockage of DNA replication, and autophagy in *A. flavus* spores. Flow cytometry analysis showed that 1-nonanol treatment caused hyperpolarization of mitochondrial membrane potential and accumulation of reactive oxygen species in *A. flavus* spores. 4′,6-diamidino-2-phenylindole staining showed that treatment with 1-nonanol destroyed the DNA. Biochemical analysis results confirmed that 1-nonanol exerted destructive effects on *A. flavus* spores by decreasing intracellular adenosine triphosphate content, reducing mitochondrial ATPase activity, accumulating hydrogen peroxide and superoxide anions, and increasing catalase and superoxide dismutase enzyme activities. This study provides new insights into the antifungal mechanisms of 1-nonanol against *A. flavus*.

Key points

- *1-Nonanol treatment resulted in abnormal morphology of A. flavus spores.*
- *1-Nonanol affects the expression of key growth-related genes of A. flavus.*
- *The apoptosis of A. favus spores were induced after exposed to 1-nonanol.*

Keywords 1-Nonanol · *Aspergillus flavus* · Transcriptomics analyses · Antifungal mechanism

Introduction

Aspergillus flavus is a common saprotrophic fungus in mildewed cereal grains and their derived foods (Liang et al. 2015; Wild and Gong 2010). The proliferation of *A. flavus* can deteriorate the quality and quantity of cereal grains and produce carcinogenic secondary metabolite aflatoxins, posing risks to human and animal health (Rocha et al. 2014). Therefore, there is a need to develop sustainable and effective measures to control *A. flavus* contamination in postharvest grains.

The application of chemical fungicides is important to control the fungal spoilage of cereal grains during

✉ Shuai-Bing Zhang
shbzhang@163.com

✉ Yuan-Sen Hu
hys308@126.com

[1] School of Biological Engineering, Henan University of Technology, 100 Lianhua Street, Zhengzhou 450001, People's Republic of China

[2] Henan Provincial Key Laboratory of Biological Processing and Nutritional Function of Wheat, Zhengzhou 450001, People's Republic of China

storage. Previously, several antifungal agents, such as propionic acid and its salts, ozone gases, and phosphine, have been used as grain protectants (Formato et al. 2011; Hardin et al. 2010; Hocking and Banks 1991; Rutenberg et al. 2018). Although antifungal agents can inhibit the growth of spoilage fungi on grain, their large-scale application is hindered by residue toxicity, fungicide resistance, and high costs (De Castro et al. 1996; Jian et al. 2013; Lorini et al. 2007). In recent years, the exploration of biofumigants from plant volatile organic compounds has attracted attention due to their natural origin, high potency, and biodegradability (Brilli et al. 2019; De Lucca et al. 2011; Hammerbacher et al. 2019; Hassanzad Azar et al. 2018; Tang et al. 2018; Wang et al. 2019; Xu et al. 2021), showing biotechnological potential for preventing fungal spoilage of agricultural products.

1-Nonanol is one of the main volatile constituents produced from cereal grains and fruits, such as wheat, cherries, and grapes (Bahena-Garrido et al. 2019; Galvão et al. 2011; Hayaloglu and Demir 2016; Mattiolo et al. 2016). 1-Nonanol can inhibit hyphal growth and spore germination in *Geotrichum candidum*, thereby preventing the development of citrus rot (Suprapta et al. 1997). Furthermore, 1-nonanol can inhibit the growth of *Zygosaccharomyces bailii* and *Saccharomyces cerevisiae* by disrupting the functions of integral proteins on the membrane (Kubo and Cespedes 2013). As a food additive approved by the National Health and Family Planning Commission of China (GB2760-2014), 1-nonanol shows potential for controlling the fungal spoilage of postharvest grains (Zhang et al. 2021a). Recently, we found that 1-nonanol could markedly inhibit *A. flavus* growth in cereal grains. It was primarily speculated that 1-nonanol treatment could cause cell membrane leakage and mitochondrial dysfunction to induce the apoptosis of *A. flavus* (Zhang et al. 2021a). However, further investigation on the antifungal mechanisms of 1-nonanol against *A. flavus* is needed.

In this study, to understand the mechanism through which 1-nonanol exerts antifungal effects against *A. flavus*, (1) the effect of 1-nonanol on the germination and microscopic morphology of *A. flavus* spores was determined; (2) transcriptomic analyses were performed to reveal changes in gene expression in *A. flavus* spores exposed to 1-nonanol; (3) the apoptosis-related characteristics of 1-nonanol-treated *A. flavus* spores, including mitochondrial membrane potential, reactive oxygen species accumulation, and DNA damage, were analyzed; (4) biochemical validation was performed to confirm the physiochemical changes between untreated and 1-nonanol-treated *A. flavus* spores. This study provides novel insights into the antifungal effects of 1-nonanol against *A. flavus*.

Materials and methods

Materials and chemicals

A. flavus NRRL3357 was conserved in our laboratory. 1-Nonanol (CAS: 205–583-7, 98%) was purchased from Macklin (Shanghai, China). Annexin V-FITC apoptosis detection, mitochondrial membrane potential (MMP), reactive oxygen species (ROS) assay kits, and 4′,6-diamidino-2-phenylindole (DAPI) were purchased from Beyotime Biotechnology (Shanghai, China). The assay kits of adenosine triphosphate (ATP), catalase (CAT), hydrogen peroxide (H_2O_2), superoxide dismutase (SOD), and superoxide anion were purchased from Solarbio Science and Technology Co. Ltd. (Beijing, China). An ATPase assay kit was purchased from the Jiancheng Bioengineering Institute (Nanjing, China).

Determination of the spore germination rate

A. flavus was cultivated on potato dextrose agar medium at 28 ± 1 ℃ for 6 days, and spores were washed with sterilized distilled water containing 0.1% Tween-80. Spore suspensions (1×10^7 spores mL^{-1}) were prepared and counted using a hemocytometer, and used for subsequent experiments. The spore germination rate of *A. flavus* was determined referring to previously reported method (Li et al. 2021; Xu et al. 2020). One milliliter of spore suspension was added to a 2-mL sterile centrifuge tube containing 1 mL of sterile yeast extract medium with supplements (YES, 2% yeast extract, 20% sucrose, and 0.05% magnesium sulfate) (Li et al. 2021), and 1-nonanol was added to generate different concentrations (0, 0.5, 1, 2, 3, and 4 μL/mL). The culture was incubated at 28 ± 1 °C and 200 rpm for 6, 12, and 24 h. The germination rate of *A. flavus* spores was calculated after microscopic observation of approximately 300 spores. The minimum concentration of 1-nonanol that totally inhibited the germination of *A. flavus* spores after 24 h of incubation was defined as the minimum inhibitory concentration (MIC). Non-germinated spores were centrifuged (6000 × *g*) and washed with 0.01 M phosphate-buffered saline (PBS, pH 7.2) and re-incubated in YES for another 24 h to determine the minimum fungicidal concentration (MFC). The inhibition ratio (IR) of germination was calculated as IR (%) = $[(G_0 - G_t)/G_0] \times 100$, where IR is the inhibition ratio of germination and G_0 and G_t is the germination rates of the control and 1-nonanol-treated spores, respectively.

Scanning electron microscopy

A. flavus spores were recovered and washed with 0.01 M PBS (pH 7.2) after treatment with 1-nonanol (0 μ L/mL,

MIC, and MFC) for 6 h. Spores were prepared for scanning electron microscopy (SEM) observation according to a previously reported method (Lv et al. 2019). First, spores were fixed with 2.5% glutaraldehyde solution, dehydrated with 30–100% ethanol solution, and resuspended in *tert*-butyl alcohol. Next, the spores were sequentially treated with an ethanol and isoamyl acetate (*V*/*V* = 1/1) mixture and isoamyl acetate. Finally, the spores were coated with gold after a critical drying process. Morphology observation of *A. flavus* spores was performed with a scanning electron microscope (Hitachi SU8010, Tokyo, Japan).

Analysis of spore apoptosis and cell membrane integrity

1-Nonanol was added to the spore suspensions in YES to obtain a final concentration of 0 μL/mL, MIC, and MFC. Cultures were incubated at 28 °C for 6 h, collected, and washed with 0.01 M PBS (pH 7.2). *A. flavus* spores were stained with the Annexin V-FITC apoptosis detection kit. The stained spores were observed with a confocal laser scanning microscope (FV3000, Olympus Corporation, Japan), and measured with a BD Accuri C6 Plus flow cytometer (Becton Dickinson, San Jose, CA, USA). Flow cytometry was used to analyze the data for at least 1×10^4 spores in each sample.

Transcriptomic analysis

A. flavus spores were collected after exposure to 0 μL/mL and MIC of 1-nonanol for 6 h. Total RNA was extracted from untreated and 1-nonanol-treated spores using the TRIzol reagent (Magen Biotechnology Co., Ltd., Guangzhou, China). RNA purity and integrity were determined as previously described (Li et al. 2021). Three micrograms of high-quality RNA was used to generate a cDNA library for sequencing using the NEBNext® UltraTM RNA Library Prep Kit for Illumina® (NEB, Ipswich, MA, USA). cDNA fragment purification, PCR, PCR product purification, and library quality evaluation were performed as described by Li et al. (2021). The clustering of index-encoded samples, the sequencing of the library, and the generation of paired-end reads were performed with reference to previous reports (Li et al. 2021). Reference genome and gene model annotation files were downloaded from the genome website (https://fungidb.org/common/downloads/Current_Release/AflavusNRRL3357/gff/data/). We used Hisat2 (2.0.5 version) (Kim et al. 2015) to construct a reference genome index and compared the double-ended clean reads with the reference genome. The mapping read for each sample was assembled using the StringTie v1.3.3b (Pertea et al. 2015). Differential expression analysis of the two groups (two biological replicates per condition) was performed using the DESeq2 R package (1.16.1) (Love et al. 2014). The resulting *P*-values were adjusted using Benjamini and Hochberg's method to control the incorrect discovery rate (Benjamini and Hochberg 1995). The identification of differentially expressed genes (DEGs), enrichment analysis of gene ontology (GO), and significant enrichment of differentially expressed genes were carried out as previously reported (Li et al. 2021). The DEG statistical enrichment test in the Kyoto Encyclopedia of Genes and Genomes (KEGG) pathway (http://www.genome.jp/kegg) was implemented using the clusterProfiler R package (Yu et al. 2012). Raw RNA-Seq data were uploaded to the NCBI Sequence Read Archive with the accession number PRJNA783782.

Real-time quantitative polymerase chain reaction validation

Total RNA was extracted from the *A. flavus* spores. First-strand cDNA was synthesized as described in our previous report (Li et al. 2021). Six representative genes were selected for PCR analysis. The primers used are listed in the supplementary material (Supplemental Table S1). The real-time quantitative polymerase chain reaction (qRT-PCR) mixture contained 10 μL 2 × Universal SYBR Green qPCR Supermix (US Everbright Inc., NJ, USA), 0.8 μL of each primer (10 Mμ), 1 μL cDNA, and 7.4 μL ddH_2O. The qRT-PCR reaction conditions were 95 °C for 120 s, 40 cycles of 95 °C for 5 s, and 60 °C for 30 s. Calculate relative gene expression using the $2^{-\Delta\Delta Ct}$ method (Livak and Schmittgen 2001).

Determination of the MMP and ROS accumulation

MMP and ROS accumulation in *A. flavus* spores were determined using a previously reported method (Li et al. 2021). The spores of *A. flavus* were exposed to 1-nonanol (0 μL/mL, MIC, and MFC), incubated at 28 °C for 6 h. The spores were collected and rinsed with 0.01 M PBS (pH 7.2). *A. flavus* spores were stained with the MMP kit and ROS assay kit, and flow cytometry was used to detect MMP and ROS accumulation.

Observation of the DNA damage

A. flavus spores were inoculated into the YES medium and exposed to 1-nonanol (0 μL/mL, MIC, and MFC) at 28 °C for 6 h. The spores was collected, and fixed in 70% ethanol (Zhang et al. 2021b). After the fixed spores were stained with 10 gμ/mL DAPI at 28 °C for 10 min, morphological changes in the *A. flavus* spore nucleus were observed by confocal laser scanning microscopy (CLSM).

Intracellular ATP, H_2O_2, and superoxide anion content, mitochondrial ATPase, CAT, and SOD activity determination

A. flavus spores were inoculated into YES medium and exposed to 0 μL/mL and MIC of 1-nonanol at 28 °C. After incubation for 6 h, spores were washed with 0.01 M PBS (pH 7.2) and collected. The intracellular ATP content was measured using an ATP content detection kit. The H_2O_2 content was determined using a hydrogen peroxide assay kit. ATPase assay kits were used to determine mitochondrial ATPase activity. Superoxide anion content was determined using a superoxide anion assay kit. SOD activity was measured using a SOD activity assay kit. The CAT activity was determined using the CAT activity assay kit.

Statistical analysis

The biochemical data were statistically analyzed using SAS 9.2 (SAS Institute, Cary, NC, USA). Statistical significance was set at $P < 0.05$. All experiments were performed in triplicate.

Results

Effects of 1-nonanol on A. flavus spore germination and morphology

The germination rate of *A. flavus* spores at 6, 12, and 24 h under different 1-nonanol concentrations was determined (Table 1). The MIC and MFC of 1-nonanol against the germination of *A. flavus* spores were 2 and 4 μL/mL, respectively. SEM observation revealed that the *A. flavus* spores without 1-nonanol treatment were normal and intact, whereas the *A. flavus* spores were wrinkled after MIC treatment or broken after MFC treatment (Fig. 1). This indicates that 1-nonanol treatment is destructive to the cell wall and membrane of *A. flavus* spores. The Annexin FITC/PI double staining was used to assess 1-nonanol-induced apoptosis and cell membrane changes of *A. flavus* spores. Annexin V specifically binds to the phosphatidylserine (PS) of the outer membrane of early apoptotic cells (Vermes et al. 1995). With the increase of 1-nonanol concentration, CLSM observed increased red and green fluorescence of *A. flavus* spores after staining, indicating that 1-nonanol destroyed the membrane integrity of *A. flavus* spores and induced their

Table 1 Effect of 1-nonanol on *A. flavus* spore germination

Spore germination (%, mean ± SD, $n = 3$)				Inhibition rate (%)	Re-cultivation in YES medium[a]
Dose (μL/mL)	6	12	24	24	
0	10.9 ± 1.6^{d}	37.8 ± 0.8^{d}	79.5 ± 1.3^{d}	0.0 ± 0.0^{f}	$+^{b}$
0.5	5 ± 0.3^{d}	22.4 ± 1.1^{e}	66.9 ± 2.3^{e}	15.6 ± 1.6^{f}	+
1	0.0 ± 0.0^{e}	0.0 ± 0.0^{f}	10.6 ± 0.5^{e}	86.7 ± 0.8^{e}	+
2	0.0 ± 0.0^{e}	0.0 ± 0.0^{f}	0.0 ± 0.0^{f}	100.0 ± 0.0^{d}	+
4	0.0 ± 0.0^{e}	0.0 ± 0.0^{f}	0.0 ± 0.0^{f}	100.0 ± 0.0^{d}	$-^{c}$

"+ b", growth. "− c", no growth; d − f, significant differences ($P < 0.05$)

[a]Re-incubated, without 1-nonanol in YES medium for 24 h to determine the MFC

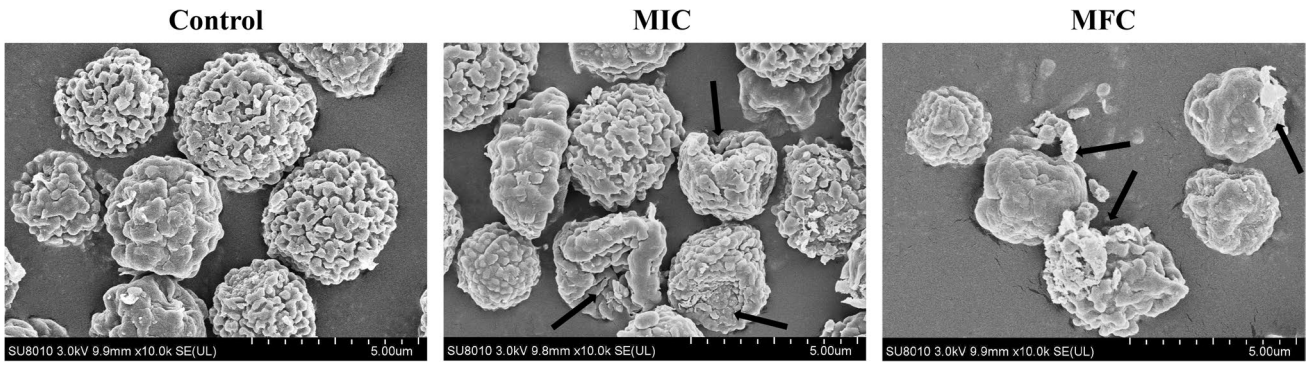

Fig. 1 SEM images of *A. flavus* spores treated with 1-nonanol for 6 h. Arrows point to wrinkled or broken surface of spores. The images represent three independent experimental replicates

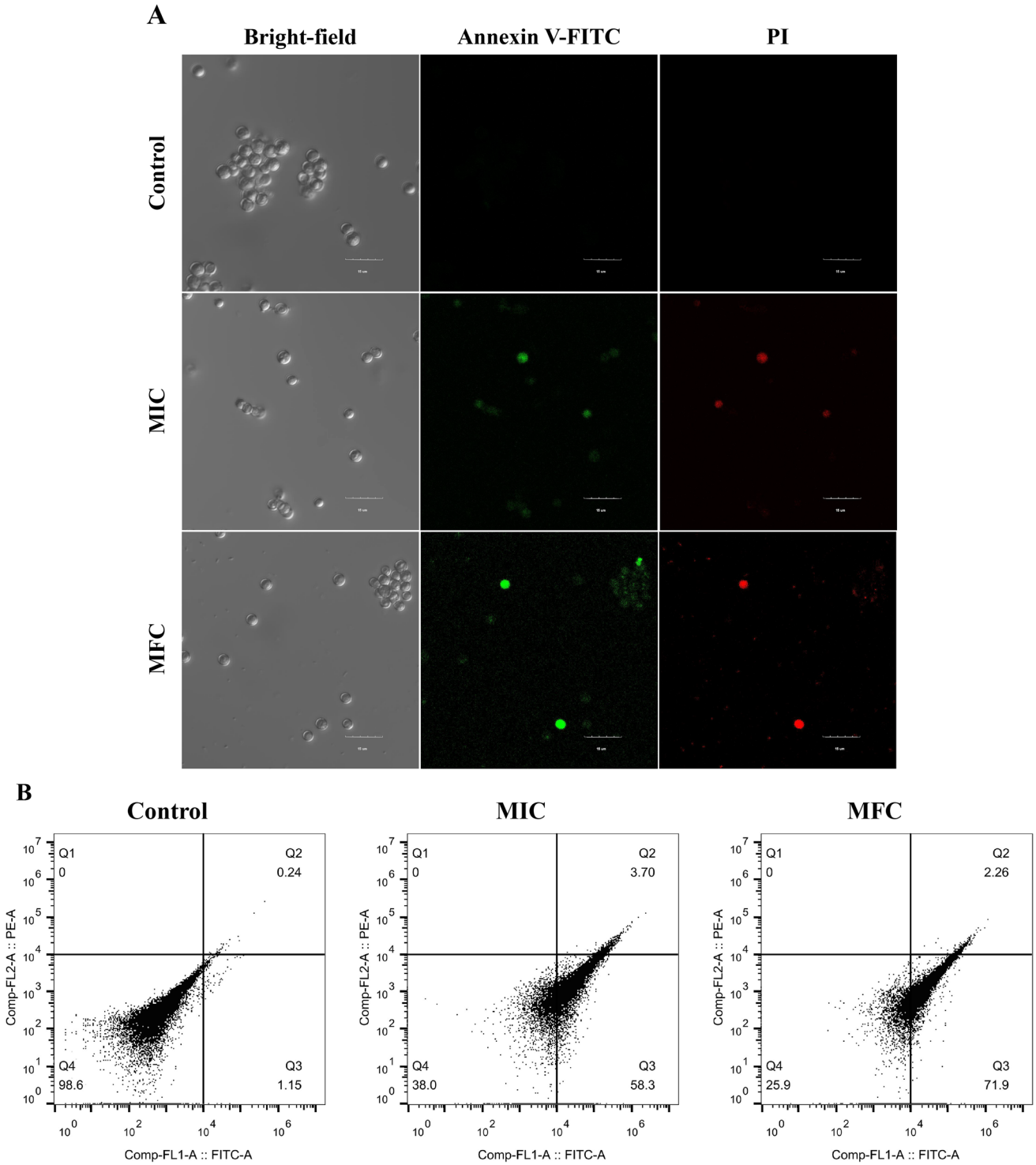

Fig. 2 Cell apoptosis and plasma membrane integrity of *A. flavus* spores analyzed with CLSM (**A**) and flow cytometry (**B**) after treatment with no 1-nonanol and its MIC and MFC for 6 h. Control, fluorescence of non-treated spores; MIC, fluorescence of spores treated with 2 μL/mL 1-nonanol; and MFC, fluorescence of spores treated with 4 μL/mL 1-nonanol. The proportion of apoptotic cells increased with 1-nonanol treatment concentration

apoptosis. Flow cytometry showed that the percentage of stained spores gradually increased from 1.15% (control) to 58.3% and 71.9% in the MIC and MFC samples, respectively (Fig. 2A, B). Furthermore, phosphatidylserine eversion and permeability of cell membrane of spores were enhanced along with the increased concentration of 1-nonanol. This

suggested that 1-nonanol could damage the cell membrane integrity of *A. flavus* spores and cause apoptosis.

Transcriptomic analysis

The DEGs between *A. flavus* spores exposed to 0 μL/mL and MIC of 1-nonanol were identified using a high-throughput RNA sequencing to reveal the molecular mechanism of 1-nonanol against *A. flavus* spores. In addition, the distribution of DEGs between the control and 1-nonanol-treated samples was visualized using a volcano plot (Supplemental Fig. S1). A total of 3,311 DEGs, including 1,897 upregulated genes and 1,414 downregulated genes, were identified between the 1-nonanol-treated and control groups. GO enrichment analysis was conducted to annotate the functional categories of DEGs between the control and 1-nonanol-treated *A. flavus* spores, including biological processes, cellular components, and molecular functions. Top ten most prominent feature entries for each category were determined (Supplemental Fig. S2), which showed that DEGs mainly included the oxidation–reduction process, organic anion transport, lipoprotein metabolic process, transition metal ion binding, oxidoreductase activity, transcription regulator activity, extrinsic component of vacuolar membrane, and Seh1-associated regulatory complex. KEGG enrichment of DEGs showed that DEGs were mainly related to membrane damage, oxidative phosphorylation, autophagy, and blockage of DNA replication (Fig. 3). According to the current analysis, 64 genes were identified as key genes (Table 2).

qRT-PCR determination of six selected genes (AFLA_136310, AFLA_004460, AFLA_106350, AFLA_079910, AFLA_050950, and AFLA_026790) was performed to validate the transcriptomic results (Supplemental Fig. S3). The expression of these six genes was consistent with the transcriptomic results.

Effect of 1-nonanol on the MMP and ROS accumulation of A. flavus spores

Flow cytometry analysis of the changes in the mitochondrial membrane potential of *A. flavus* was conducted after treatment with 0 μL/mL, MIC, and MFC of 1-nonanol (Fig. 4). In the experiment, Q2 and Q3 represent the proportion of *A. flavus* spores containing and without MMP, respectively. With an increase in 1-nonanol concentration, the fluorescence signal of the Q2 area increased from 46.2 to 87.0% and 91.0%, while the fluorescence signal of the Q3 area decreased from 39.1 to 12.2% and 8.14%. This indicated that 1-nonanol treatment increased the MMP of *A. flavus* spores. Therefore, 1-nonanol treatment increased the MMP of *A. flavus* spores and caused its MMP hyperpolarization. ROS accumulation test results showed that only 13.3% of the control group showed ROS-specific fluorescence, while these values in the 1-nonanol MIC and MFC treatment groups were 57.2% and 68.2%, respectively (Fig. 5).

Effects of 1-nonanol on DNA fragmentation

DAPI staining showed that the DNA fragmentation fluorescence intensity of the 1-nonanol-treated group was markedly enhanced compared to that of the control group in a dose-dependent manner (Fig. 6). These findings indicate that treatment with 1-nonanol damages the DNA of *A. flavus* spores.

Biochemical validation

The intracellular ATP content and mitochondrial ATPase activity in *A. flavus* cells treated with 1-nonanol decreased by 47.45% and 52.41%, respectively, relative to the control (Fig. 7A, B). H_2O_2 content and CAT activity in *A. flavus* spores treated with 1-nonanol increased by 61.54% and 31.43%, respectively, relative to the control (Fig. 7C, D). Superoxide anion content and SOD activity in cells with 1-nonanol treated were enhanced by 59.56% and 69.60%, respectively, relative to the control (Fig. 7E, F).

Discussion

As a natural plant volatile matter and authorized food additive, 1-nonanol shows potential for use as a bio-preservative for postharvest management (Zhang et al. 2021a). In this study, we investigated the antifungal mechanism of 1-nonanol against *A. flavus* at the molecular level. 1-Nonanol has a high inhibitory activity against the germination of *A. flavus* spores. Transcriptional profile analysis showed that 1-nonanol treatment mainly affected the expression of genes related to membrane damage, oxidative phosphorylation, autophagy, and blockage of DNA replication in *A. flavus* spores. In addition, 1-nonanol treatment could induce apoptosis in *A. flavus* spores. The physiological and biochemical effects of 1-nonanol against *A. flavus* spores were validated.

Cell wall and cell membrane integrity

Apoptosis is the process of programed cell death, accompanied by physiological changes, such as abnormal morphology, PS externalization, abnormal MMP, and DNA decomposition (Sharon et al. 2009). 1-Nonanol can damage the cell wall of *A. flavus* spores. The cell wall is a barrier that protects the fungus from adverse effects (Free 2013). From the SEM results, breakage of the cell wall of spores exposed to 1-nonanol could be observed. Destruction of the cell wall

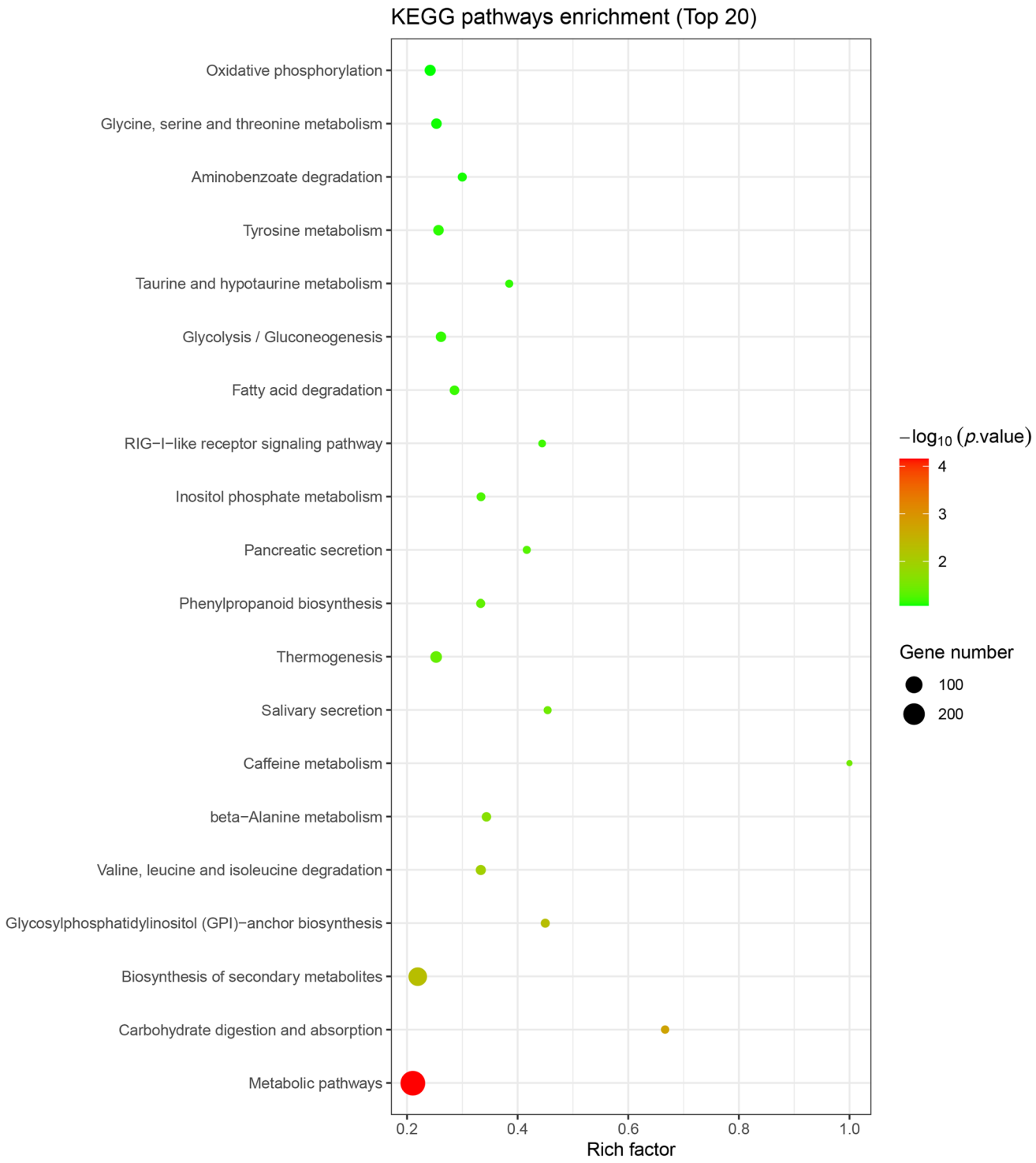

Fig. 3 KEGG pathways showing enrichment of DEGs between the 1-nonanol-treated and control groups

structure causes cell membrane rupture and cell lysis, affecting the survival of fungal cells (Cortés et al. 2019). Chitin is the main component of fungal cell walls and the reduction in its biomass results in a decline in cell viability (Free 2013). In this study, four chitinase-related genes (AFLA_101800, AFLA_031380, AFLA_028280, and AFLA_104680) were upregulated in *A. flavus* spores after 1-nonanol treatment. Chitinase is an extracellular enzyme complex that degrades chitin. Upregulation of the gene encoding chitinase degrades the chitin present in *A. flavus* spores and affects the integrity

Table 2 Representative DEGs from different comparisons of spore after 1-nonanol-treatment and control. C: control; T: 1-nonanol treatment; FDA: corrected *P*-value

Gene ID	Log2 FC (T vs C)	Name	*P*-value	FDA	Description
AFLA_101800	2.0415		5.77E-06	2.03E-05	Class III chitinase
AFLA_031380	1.5938		1.00E-199	6.42E-198	Class V chitinase
AFLA_042780	1.2679		1.85E-91	5.47E-90	Chitin synthase A
AFLA_072370	1.3588		0.00010113	0.0003099	Hexokinase
AFLA_135190	4.1809		0	0	Cytochrome b5 reductase
AFLA_114760	1.129		4.63E-26	4.80E-25	Chitin synthase B
AFLA_028280	2.5982		0.0020911	0.0052657	Symbiotic chitinase
AFLA_087870	1.1309		0.0010432	0.0027591	Endoglucanase
AFLA_036130	− 1.7997	*Cyp51A*	5.356E-22	4.9189E-21	14-α-Sterol demethylase
AFLA_001030	3.4591	*Erg7*	5.09E-19	4.16E-18	Lanosterol synthase
AFLA_051080	− 1.34		2.07E-15	1.42E-14	C-14 sterol reductase
AFLA_121580	− 2.9102		7.91E-150	3.84E-148	C-4 methyl sterol oxidase
AFLA_138060	− 1.1722	*Erg4*	0.022133	0.045272	C-24 (28) sterol reductase
AFLA_021770	− 2.1438		0.0060358	0.013977	Tocopherol-*O*-methyltransferase
AFLA_111350	− 1.923		5.74E-51	1.02E-49	C-14 sterol reductase
AFLA_061500	− 0.6129	*Erg1*	1.04E-13	6.51E-13	Squalene mono oxygenase
AFLA_m0030	4.1886		1.10E-121	4.46E-120	NADH dehydrogenase subunit 1
AFLA_m0460	4.0363		6.20E-151	3.02E-149	NADH dehydrogenase subunit 2
AFLA_m0410	4.0308		4.39E-170	2.39E-168	NADH dehydrogenase subunit 3
AFLA_m0060	3.6895		8.38E-160	4.33E-158	NADH dehydrogenase subunit 4
AFLA_m0450	4.1119		0	0	NADH dehydrogenase subunit 5
AFLA_m0130	3.338		5.51E-11	2.91E-10	NADH dehydrogenase subunit 6
AFLA_m0440	4.8306		7.98E-50	1.39E-48	NADH dehydrogenase subunit 4L
AFLA_m0380	4.3882		0	0	Cytochrome oxidase subunit 1
AFLA_m0420	4.2071		5.58E-102	1.86E-100	Cytochrome oxidase subunit 2
AFLA_m0140	4.1189		0	0	Cytochrome oxidase subunit 3
AFLA_m0010	4.0349		7.55E-276	7.55E-276	Cytochrome b
AFLA_135090	− 1.4184	*Cox11*	5.06E-09	2.33E-08	Cytochrome c oxidase assembly protein
AFLA_077210	1.5305		3.08E-09	1.43E-08	NADPH:FDA oxidoreductase
AFLA_108790	− 1.1461	*AldA*	1.27E-73	3.10E-72	Aldehyde dehydrogenase
AFLA_115890	2.7811		0.0013343	0.0034713	Acyl-CoA oxidase
AFLA_077410	− 1.764		6.80E-07	2.61E-06	Acyl-CoA dehydrogenase
AFLA_026790	− 1.1771	*PpoA*	1.48E-89	4.30E-88	Fatty acid oxygenase
AFLA_004460	− 1.5255		2.59E-156	1.31E-154	Fatty acid desaturase family protein
AFLA_004970	− 0.8525	*Gns1*	4.45E-08	1.89E-07	Fatty acid elongase
AFLA_073840	− 1.1481		0.00028553	0.00082328	Na/K ATPase α 1 subunit
AFLA_081310	− 2.522		4.35E-24	4.27E-23	ATP-dependent Clp protease
AFLA_080240	− 0.6464		7.99E-17	5.90E-16	ATP synthase δ chain, mitochondrial precursor
AFLA_035290	1.0915		1.40E-189	8.53E-188	Pyruvate dehydrogenase
AFLA_007020	0.5438	*Cit1*	1.10E-85	3.06E-84	Citrate synthase
AFLA_106350	− 0.9106	*Acl*	2.00E-52	3.61E-51	ATP citrate lyase subunit
AFLA_086400	− 1.0559	*Idp1*	2.24E-50	3.94E-49	Isocitrate dehydrogenase
AFLA_015810	1.8146		6.79E-33	6.79E-33	Citrate synthase
AFLA_096210	1.0714		1.14E-123	4.69E-122	Catalase
AFLA_034380	0.2556		5.16E-09	2.37E-08	Catalase
AFLA_033420	2.3772	*MnSOD*	4.59E-35	6.07E-34	Mn superoxide dismutase
AFLA_079910	2.1819	*Hyr1*	0	0	Glutathione peroxidase
AFLA_045990	− 1.255	*Cdc9*	3.47E-11	1.86E-10	DNA ligase

Table 2 (continued)

Gene ID	Log2 FC (T vs C)	Name	*P*-value	FDA	Description
AFLA_085970	− 1.2471	*Pri1*	0.013356	0.028831	DNA primase subunit
AFLA_054950	− 1.1982	*Rfc4*	6.98E-11	3.66E-10	DNA replication factor C subunit
AFLA_028600	− 1.3588	*Mcm3*	7.26E-07	2.78E-06	DNA replication licensing factor
AFLA_045950	− 1.0121	*Mcm4*	0.000071846	0.00022401	DNA replication licensing factor
AFLA_004710	− 0.8827	*Mcm5*	0.0047201	0.011164	DNA replication licensing factor
AFLA_129000	1.0558	*Apg12*	1.37E-17	1.05E-16	Autophagy protein
AFLA_126850	3.7674	*Pep4*	0.0026913	0.0066563	Vacuolar protease A
AFLA_110620	1.0245	*Pdd7p*	1.57E-98	4.96E-97	Serine/threonine protein kinase
AFLA_104050	0.6622	*Atg4*	1.45E-27	1.56E-26	Autophagy cysteine endopeptidase
AFLA_021590	0.4441	*Vtc1*	9.57E-08	3.95E-07	Vacuolar transporter chaperon
AFLA_132710	− 1.2116		1.70E-10	8.71E-10	TFIID and SAGA complex TAF10 subunit
AFLA_007150	− 1.5961	*Ssl1*	1.98E-12	1.15E-11	RNA polymerase TFIIH complex subunit
AFLA_046540	− 1.7232		5.72E-16	4.03E-15	Transcription factor TFIIE complex alpha subunit
AFLA_132860	− 1.1129	*Tfb4*	1.84E-18	1.47E-17	Transcription factor TFIIH subunit
AFLA_080590	− 1.0827		2.26E-18	1.79E-17	Transcription initiation factor TFIID subunit
AFLA_017520	− 2.2384	*Rad3*	1.21E-39	1.77E-38	TFIIH complex helicase

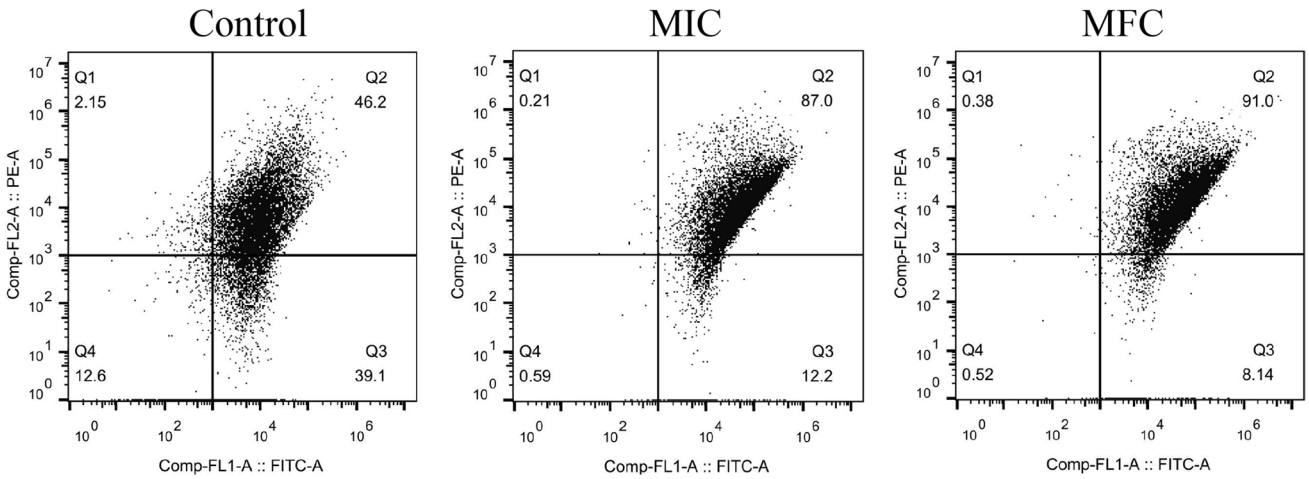

Fig. 4 Changes in MMP of *A. flavus* spores exposed to 1-nonanol. Control, MIC, and MFC; fluorescence of untreated and 1-nonanol-treated (2 and 4 μL/mL, respectively) spores. Fluorescence migration from Q3 to Q2 with increasing 1-nonanol concentration

of the cell wall. Interestingly, genes encoding chitin synthase A (AFLA_042780) and chitin synthase B (AFLA_114760) were also upregulated in 1-nonanol-treated *A. flavus* spores. These DEGs indicate that 1-nonanol can change the properties of *A. flavus* cell walls while triggering a genetic compensation response (GCR) to cell wall damage. It has been reported that yeast cells upregulate the expression of genes related to cell wall biogenesis to overcome the damage caused by terpenes (Parveen et al. 2004). Although current evidence indicates that 1-nonanol has multiple effects on the *A. flavus* spore cell wall, since the surface of the conidia is a relatively rigid structure, it is still unclear how 1-nonanol can change the morphology of the conidia.

1-Nonanol treatment also disrupted the cell membrane of *A. flavus* cells. The results of Annexin V-FITC staining indicated that 1-nonanol treatment could cause PS externalization in the plasma membrane of *A. flavus* spores, which is typical biochemical marker of fungal cell (Ma et al. 2017). Propidium iodide staining indicated that 1-nonanol treatment increased membrane permeability of *A. flavus* spores. This supported our previous speculation that 1-nonanol treatment increases the

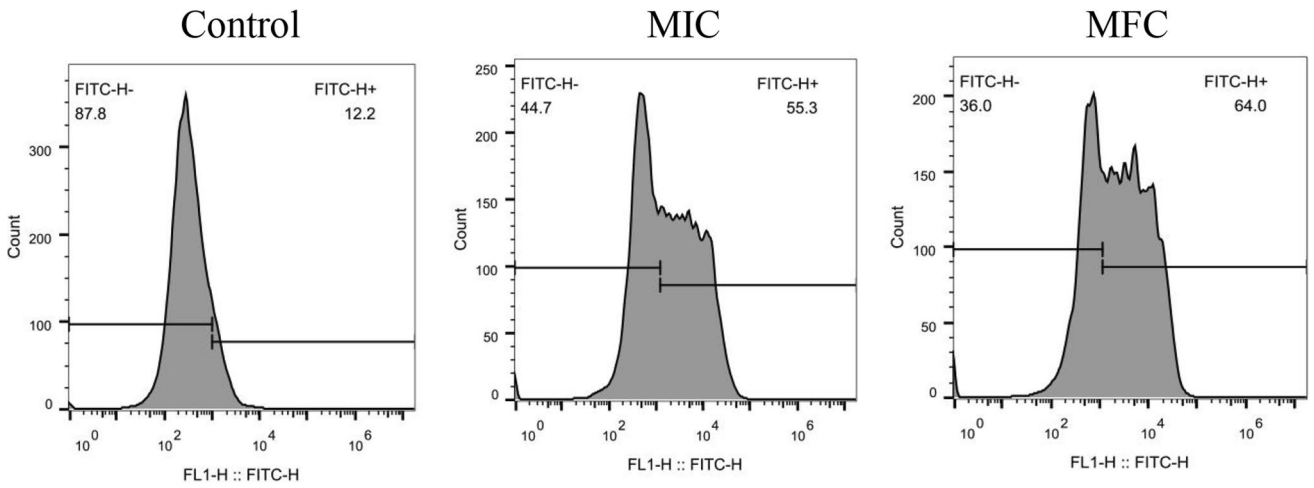

Fig. 5 Endogenous ROS accumulation of *A. flavus* spores exposed to 1-nonanol. Control, MIC, and MFC; fluorescence of non-treated and 1-nonanol-treated (2 and 4 μL/mL, respectively) spores. Fluorescence increased with increasing 1-nonanol treatment concentration

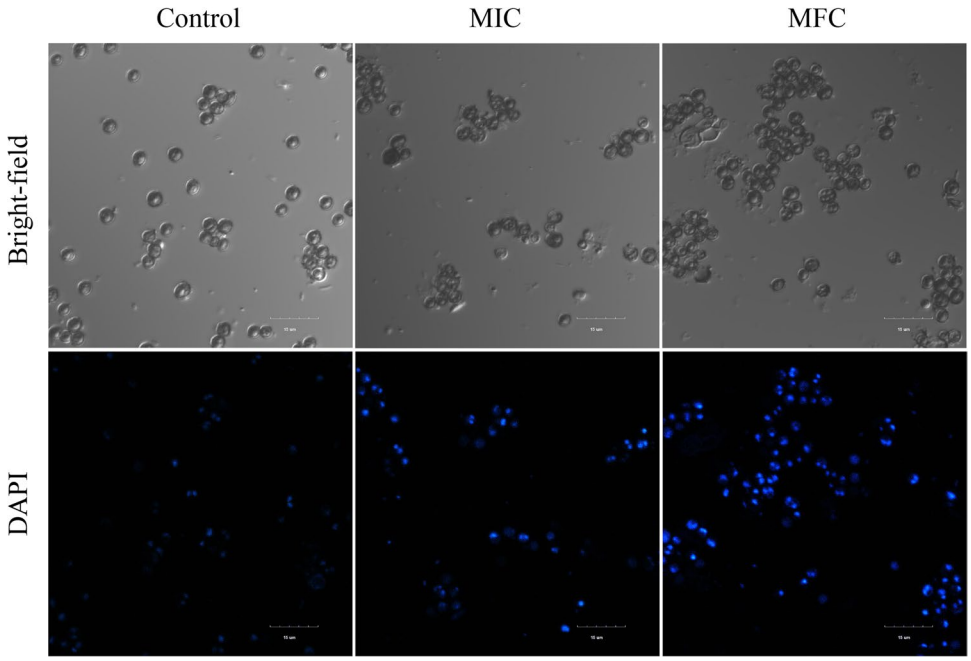

Fig. 6 DNA fragmentation in *A. flavus* spores exposed to 1-nonanol observed by CLSM. Control, MIC, and MFC; fluorescence of non-treated and 1-nonanol-treated (2 and 4 μL/mL, respectively) spores. Fluorescence increased with increasing 1-nonanol concentration

permeability of the cell membrane of *A. flavus* (Zhang et al. 2021a). Microbial cells respond to environmental pressure by adjusting the ratio of saturated fatty acids to unsaturated fatty acids (Wu et al. 2012). This study found that three genes related to fatty acid metabolism were downregulated after 1-nonanol treatment. *Gns1* encodes fatty acid elongase and participates in the biosynthesis of polyunsaturated fatty acids. Two genes, *PpoA*, AFLA_026790, and AFLA_004460, encoding the fatty acid oxygenase and desaturase, respectively, catalyze the desaturation of oleic acid to linoleic acid. The downregulation of these genes would alter the metabolic pathway of fatty acids in *A. flavus* cell, eventually affecting the synthesis of cell membrane fatty acids. In *Botrytis cinerea* cells treated with tea tree oil (TTO) and its two characteristics, genes involved in fatty acid biosynthesis were downregulated, affecting the composition of the cell membranes (Li et al. 2020). Ergosterol is the main component of fungal cell membranes and affects membrane permeability and membrane-bound enzyme activity (Chen et al. 2018). Transcriptomic analysis revealed that genes related to the ergosterol synthesis pathway were differentially expressed after 1-nonanol treatment. However, only the lanosterol synthase (*Erg7*, AFLA_001030) gene

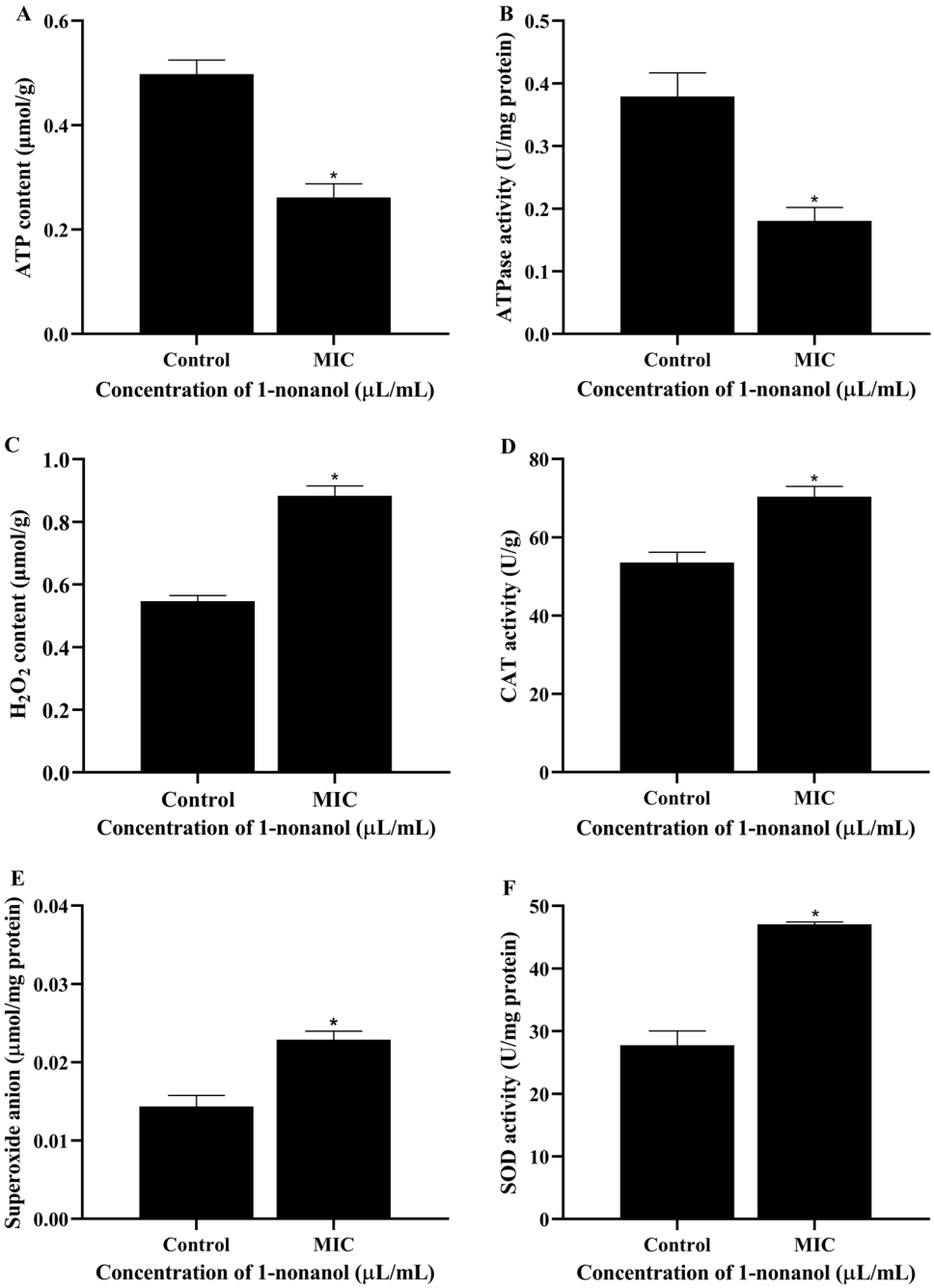

Fig. 7 Changes in intracellular ATP content (**A**), mitochondrial ATPase activity (**B**), H_2O_2 content (**C**), CAT activity (**D**), superoxide anion content (**E**), SOD activity (**F**) in the *A. flavus* spores exposed to 1-nonanol. Data are presented as the mean ± SD ($n = 3$). The asterisk indicates significant differences, $^*P < 0.05$

was upregulated and its downstream genes were downregulated (AFLA_051080; *Cyp51A*, AFLA_036130; AFLA_121580; *Erg4*, AFLA_138060; AFLA_021770; *Erg1*, AFLA_061500; and AFLA_111350). *Erg4* catalyzes the last step in the ergosterol synthesis pathway. We speculate that 1-nonanol treatment reduced the biosynthesis of ergosterol in *A. flavus* spores and changed membrane fluidity. It was previously reported that TTO treatment reduced ergosterol in *B. cinerea* and *Penicillium expansum*, increased membrane permeability, and caused mycelial death (Li et al. 2017a).

Mitochondrial dysfunction and energy supply

Our previous study speculated that 1-nonanol treatment might cause mitochondrial dysfunction of *A. flavus* cells. In this study, we provided more evidence to confirm that *A. flavus* mitochondria is a potential antifungal target of 1-nonanol. Increased intracellular ROS levels and MMP hyperpolarization supported mitochondrial dysfunction in 1-nonanol-treated *A. flavus* spores (Zorova et al. 2018), which were also found in *Rhizopus stolonifer* treated with thymol and salicylic acid (Kong et al. 2019). 1-Nonanol treatment

impairs the mitochondrial respiratory chain of *A. flavus* spores. The inner membrane of eukaryotic mitochondria is the main site of oxidative phosphorylation, which can form a proton gradient, and finally convert ADP to ATP through the respiratory chain (Chaban et al. 2014; Mitchell 1961). In this study, 9 DEGs related to oxidative phosphorylation were found in the 1-nonanol treatment and control groups. Seven genes encoding NADH dehydrogenase subunits (AFLA_m0030, AFLA_m0460, AFLA_m0410, AFLA_m0060, AFLA_m0450, AFLA_m0130, and AFLA_m0440) were upregulated in 1-nonanol-treated cells. NADH dehydrogenase subunits were involved in the composition of mitochondrial complex I (Bridges et al. 2010). Genes encoding cytochrome b (AFLA_m0010) were upregulated in *A. flavus* spores exposed to 1-nonanol. Cytochrome b was involved in the composition of mitochondrial complex III (Calderon et al. 2013). However, genes encoding the cytochrome c oxidase assembly protein (*Cox11*, AFLA_135090) were downregulated. Cytochrome c oxidase catalyzes the end step of the electron transport chain of cellular respiration (Li et al. 2006). We speculate that 1-nonanol treatment affects the end of the electron transport chain and stimulate the occurrence of GCR to maintain the mitochondrial electron transport chain. The differential expression of these genes may reduce ATP production. Furthermore, the verification experiment showed that the cell ATP content decreased, which confirmed our speculation. Therefore, 1-nonanol treatment could disrupt the respiratory chain of *A. flavus* spore mitochondria, resulting in an imbalance energy supply. A similar mechanism of respiratory chain damage was also observed in *Penicillium italicum* exposed to flavonoids from *Sedum aizoon* L. (Luo et al. 2020).

1-Nonanol treatment reduced the mitochondrial ATPase activity of *A. flavus* spores and interfered with the tricarboxylic acid cycle (TCA), impairing the mitochondrial energy supply. ATPase is a globular protein that maintains cell metabolism and viability and releases intracellular energy (Hu et al. 2021). In the current study, two genes encoding the Na/K ATPase α 1 subunit and ATP-dependent Clp protease (AFLA_073840 and AFLA_081310) were downregulated in the 1-nonanol-treated group. The downregulation of these two genes at the molecular level verified our previous study that 1-nonanol treatment reduced the mitochondrial ATPase activity of *A. flavus* (Zhang et al. 2021a). Essential oils from *Perilla frutescens* and oregano also caused reduction of ATPase activity in *A. flavus* and *Staphylococcus aureus* (Cui et al. 2019; Hu et al. 2021). In addition, verification experiments showed that 1-nonanol treatment reduced mitochondrial ATPase activity, suggesting that the energy supply of mitochondria was disrupted. Mitochondria produce ATP through TCA cycle and oxidative phosphorylation to provide energy for cells (Vakifahmetoglu-Norberg et al. 2017). Furthermore, four DEGs related to the TCA cycle were enriched, in which three genes encoding pyruvate dehydrogenase and citrate synthase (AFLA_035290; *Cit1*, AFLA_007020; and AFLA_007020, respectively) were upregulated, and the gene encoding isocitrate dehydrogenase (*Idp1*, AFLA_086400) were downregulated. Pyruvate dehydrogenase catalyzes the production of acetyl-CoA from pyruvate produced by glycolysis. Citrate synthase is the first enzyme in the TCA cycle, performing the irreversible condensation of acetyl-CoA and oxaloacetate to form citrate (Ciccarone et al. 2019). Isocitrate dehydrogenase catalyzes the removal of two hydrogens from isocitrate, and one of them is transferred to the carrier NAD in the form of a hydride, which then powers the rotation of ATP synthase (Zheng and Jia 2010). Exposure to 1-nonanol could interfere with the third step of the TCA cycle and stimulate *A. flavus* spores to upregulate genes related to the production of acetyl-CoA and citric acid to maintain energy supply. These results suggest that 1-nonanol treatment could interfere with the TCA cycle and impair mitochondrial energy supply. It was reported that TTO exposure disrupted the TCA cycle of *B. cinerea*, resulting in cell death (Xu et al. 2017; Li et al. 2017b; Wang et al. 2021).

Protective antioxidant mechanisms, block of DNA replication, and autophagic pathway

ROS are by-products of oxidative phosphorylation in the mitochondria. Environmental stress would cause the accumulation of intracellular ROS, causing mtDNA damage and lipid peroxidation (Papoutsis et al. 2019). Our previous reported that 1-nonanol-treated would cause the accumulation of H_2O_2 and superoxide anions in the *A. favus* hyphae, and cause an oxidative burst. Here, flow cytometry and validation experiments provide more evidence that 1-nonanol treatment can cause ROS accumulation in *A. flavus* cells. Eukaryotes activate defense mechanisms to protect cells from damage caused by drastic changes in the environment (Li et al. 2011). The degree of cellular oxidative stress is determined by the balance between the production of reactive oxygen species and antioxidant defense capabilities (Cesaratto et al. 2004). In this study, three genes encoding peroxisomes were differentially expressed. Genes encoding catalase (AFLA_096210 and AFLA_034380) and manganese superoxide dismutase (*MnSOD*, AFLA_033420) were upregulated. Catalase catalyzes H_2O_2 into water and oxygen, while MnSOD maintains a low steady-state concentration of superoxide anion in the cell (Candas and Li 2014; Ho et al. 2004). Validation experiments showed that treatment with 1-nonanol can increased the activities of catalase and superoxide dismutase. The upregulation of genes related to antioxidant enzyme activity and the increase of enzyme activity suggest that 1-nonanol treatment stimulated the protective antioxidant mechanism of *A. flavus* spores. Similarly,

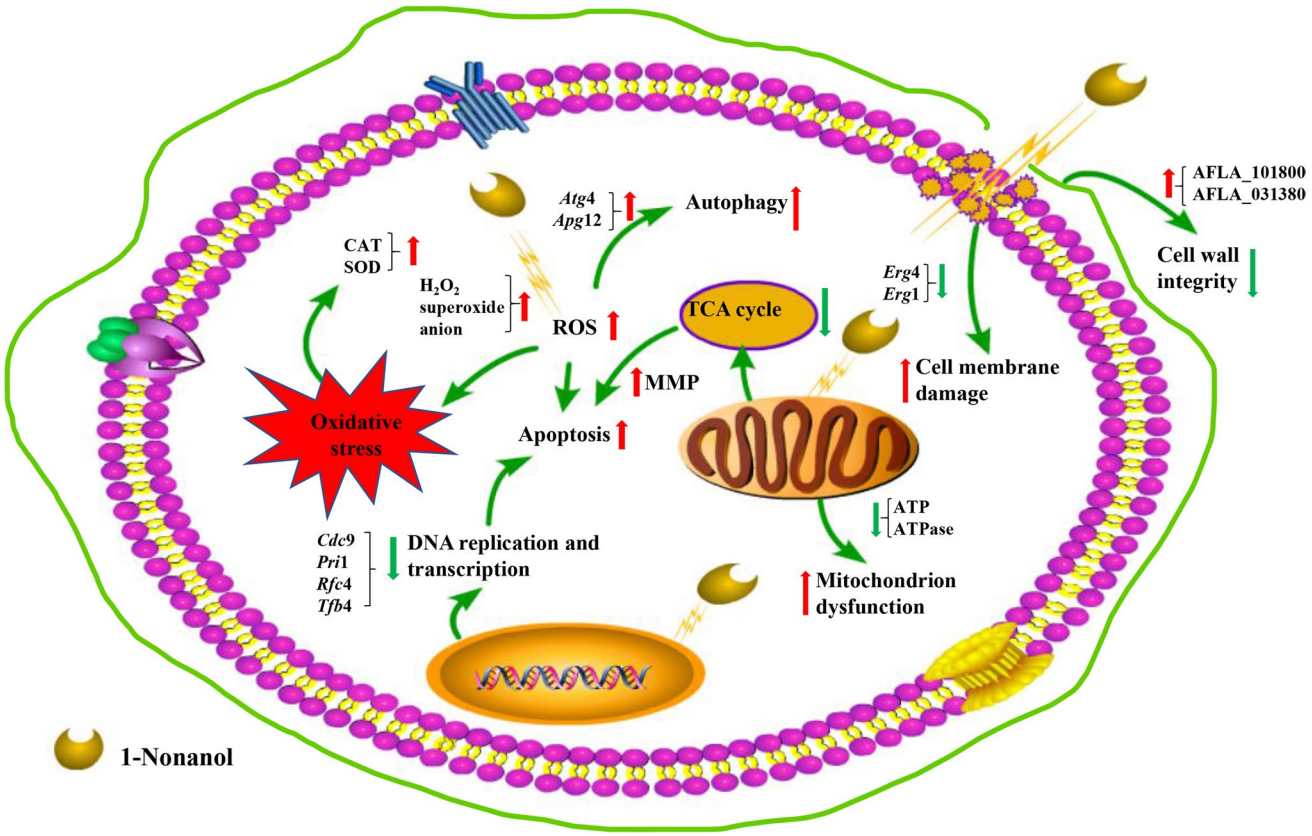

Fig. 8 Model diagram of the mechanism through which 1-nonanol exerts inhibitory effects against *A. flavus*

peptide MAF-1 treatment induced over-expression of *C. albicans* oxidative stress-related genes *CAT1*, *YBH1*, and *SOD* to protect it from ROS (Wang et al. 2017).

DAPI staining showed that 1-nonanol treatment increased the fragmentation fluorescence intensity of *A. flavus* spores compared to the control group, indicating that 1-nonanol could damage the nuclei of *A. flavus* spores. In the current study, we found that 1-nonanol treatment can inhibit the DNA replication of *A. flavus* spores. The genes encoding DNA ligase and DNA primase subunit (*Cdc9*, AFLA_045990; and *Pri1*, AFLA_085970), two key enzymes involved in DNA replication pathways, were downregulated. The cell cycle mutant *Cdc9* in *S. cerevisiae* is defective in DNA ligase and cannot repair damaged DNA caused by methyl methane-sulfonate (Johnston 1979). In addition, three genes encoding the DNA replication licensing factor (*Mcm3*, AFLA_028600; *Mcm4*, AFLA_045950; and *Mcm5*, AFLA_004710, respectively) and the gene encoding the DNA replication factor C (RFC) subunit (*Rfc4*, AFLA_054950) were downregulated. The Mcm protein family consists of six related proteins (Mcm 2–7), helicases necessary for eukaryotic DNA replication (Forsburg 2004). The RFC is a multiprotein complex of five different polypeptides (RFC 1–5). During DNA synthesis, RFC assembles the proliferation cell nuclear antigen (PCNA) on the leading and lagging strands, and then the PCNA interacts with the DNA polymerases ε and δ, respectively, to initiate progressive DNA synthesis (Wen et al. 2018; Strzalka and Ziemienowicz 2011). Therefore, inhibition of the expression of *Mcm3*, *Mcm4*, *Mcm5*, and *Rfc4* interferes with normal DNA replication. The antifungal effect exhibited by 1-nonanol by blocking DNA replication is similar to miconazole analogs (Zhang et al. 2017).

Autophagy plays an important role in the maintenance of normal cell physiology. It maintains homeostasis by digesting dysfunctional organelles and protein aggregates to prevent cellular stress (Denton et al. 2020). The autophagy pathway is activated following exposure to environmental pressures. ROS are signaling molecules in various pathways that regulate cell survival and death and can induce autophagy through several different mechanisms involving *Atg4*, catalase, and the mitochondrial electron transport chain (Azad et al. 2009). 1-Nonanol treatment upregulated the expression of five genes (*Apg12*, *Atg4*, *Pdd7p*, *Vtc1*, and *Pep4*) related to the autophagy regulatory pathway, thus indicating that the autophagy pathway was activated. However, activation of autophagy poses a potential risk. Autophagy may help save dying

cells and kill viable cells (Levine and Kroemer 2008). We speculate that when *A. flavus* spores respond to oxidative stress induced by 1-nonanol, the antioxidant pathway is activated and the level of autophagy increases to help cells maintain their stability. However, excessive defense mechanisms may lead to defensive dysfunction and aggravate the cell damage caused by oxidative stress.

In conclusion, we propose a hypothetical model of the antifungal mechanism of 1-nonanol against *A. flavus* (Fig. 8). 1-Nonanol blocks cell integrity, oxidative phosphorylation, and mitochondrial function genes. Furthermore, it interferes with the processes of genetic information transmission, such as DNA replication and transcription, inducing antioxidant pathways and autophagy, causing mitochondrial dysfunction, and eventually leading to cell death.

Supplementary Information The online version contains supplementary material available at https://doi.org/10.1007/s00253-022-11830-4.

Author contribution Y. L. Q.: experimentation; writing—original draft; investigation. S. B. Z.: supervision; data curation; writing—review and editing; resources. Y. Y. L.: software, visualization. H. C. Z.: software, validation. Y. S. H.: visualization, conceptualization, validation. J. P. C.: methodology, conceptualization.

Funding This work was supported by the National Natural Science Foundation of China (grant number 31772023), the National Key Research and Development Plan of China (grant number 2019YFC1605303-04), the Scientific and Technological Research Project of Henan Province (grant number 212102110193), the Natural Scientific Research Innovation Foundation of Henan University of Technology (grant number 2020ZKCJ01), the Cultivation Programme for Young Backbone Teachers in Henan University of Technology, and the Scientific Research Foundation of Henan University of Technology (grant number 2018RCJH14).

Data availability The datasets generated during and/or analyzed during the current study are available from the corresponding author on reasonable request.

Declarations

Ethical approval This article does not contain studies conducted on human participants or animals by any of the authors.

Conflict of interest The authors declare no competing interests.

Reference

Azad MB, Chen Y, Gibson SB (2009) Regulation of autophagy by reactive oxygen species (ROS): implications for cancer progression and treatment. Antioxid Redox Sign 11(4):777–790. https://doi.org/10.1089/ars.2008.2270

Bahena-Garrido SM, Ohama T, Suehiro Y, Hata Y, Isogai A, Iwashita K, Goto-Yamamoto N, Koyama K (2019) The potential aroma and flavor compounds in *Vitis* sp. cv. Koshu and *V. vinifera* L. cv. Chardonnay under different environmental conditions. J Sci Food Agric 99(4):1926–1937. https://doi.org/10.1002/jsfa.9389

Benjamini Y, Hochberg Y (1995) Controlling the false discovery rate: a practical and powerful approach to multiple testing. J R Stat Soc B 57(1):289–300. https://doi.org/10.1111/j.2517-6161.1995.tb02031.x

Bridges HR, Fearnley IM, Hirst J (2010) The subunit composition of mitochondrial NADH: ubiquinone oxidoreductase (complex I) from *Pichia pastoris*. Mol Cell Proteomics 9(10):2318–2326. https://doi.org/10.1074/mcp.M110.001255

Brilli F, Loreto F, Baccelli I (2019) Exploiting plant volatile organic compounds (VOCs) in agriculture to improve sustainable defense strategies and productivity of crops. Front Plant Sci 10:264. https://doi.org/10.3389/fpls.2019.00264

Calderon F, Wilson DM, Gamo FJ (2013) Antimalarial drug discovery: recent progress and future directions. Prog Med Chem 52:97–151. https://doi.org/10.1016/B978-0-444-62652-3.00003-X

Candas D, Li JJ (2014) MnSOD in oxidative stress response-potential regulation via mitochondrial protein influx. Antioxid Redox Sign 20(10):1599–1617. https://doi.org/10.1089/ars.2013.5305

Cesaratto L, Vascotto C, Calligaris S, Tell G (2004) The importance of redox state in liver damage. Ann Hepatol 3(3):86–92. https://doi.org/10.1016/s1665-2681(19)32099-x

Chaban Y, Boekema EJ, Dudkina NV (2014) Structures of mitochondrial oxidative phosphorylation supercomplexes and mechanisms for their stabilisation. Biochim Biophys Acta 1837(4):418–426. https://doi.org/10.1016/j.bbabio.2013.10.004

Chen Y, Zhang X, Zhang M, Zhu J, Wu Z, Zheng X (2018) A transcriptome analysis of the ameliorate effect of *Cyclocarya paliurus* triterpenoids on ethanol stress in *Saccharomyces cerevisiae*. World J Microb Biot 34(12):182. https://doi.org/10.1007/s11274-018-2561-1

Ciccarone F, Di Leo L, Ciriolo M R (2019) TCA cycle aberrations and cancer. In: Boffetta P and Hainaut P (ed), Encyclopedia of cancer, 3rd edn. Academic Press. pp 429–436. https://doi.org/10.1016/B978-0-12-801238-3.65066-3

Cortés JCG, Curto MA, Carvalho VSD, Pérez P, Ribas JC (2019) The fungal cell wall as a target for the development of new antifungal therapies. Biotechnol Adv 37(6):107352. https://doi.org/10.1016/j.biotechadv.2019.02.008

Cui H, Zhang C, Li C, Lin L (2019) Antibacterial mechanism of oregano essential oil. Ind Crop Prod 139(8):111498. https://doi.org/10.1016/j.indcrop.2019.111498

De Castro MFPPM, Pacheco IA, Soares LMV, Furlani RPZ, De Paula DC, Bolonhezi S (1996) Warehouse control of *Aspergillus flavus* Link and *A. parasiticus* speare on peanuts (*Arachis hypogaea*) by phosphine fumigation and its effect on aflatoxin production. J Food Protect 59(4):407–411. https://doi.org/10.4315/0362-028X-59.4.407

De Lucca AJ, Carter-Wientjes CH, Boué S, Bhatnagar D (2011) Volatile *trans*-2-hexenal, a soybean aldehyde, inhibits *Aspergillus flavus* growth and aflatoxin production in corn. J Food Sci 76(6):M381–M386. https://doi.org/10.1111/j.1750-3841.2011.02250.x

Denton D, O'Keefe L, Kumar S (2020) *Drosophila* as a model to understand autophagy deregulation in human disorders. Prog Mol Biol Transl Sci 172:375–409. https://doi.org/10.1016/bs.pmbts.2020.01.005

Formato A, Naviglio D, Pucillo GP, Nota G (2011) Improved fumigation process for stored foodstuffs by using phosphine in sealed chambers. J Agr Food Chem 60(1):331–338. https://doi.org/10.1021/jf204323s

Forsburg SL (2004) Eukaryotic MCM proteins: beyond replication initiation. Microbiol Mol Biol R 68(1):109–131. https://doi.org/10.1128/MMBR.68.1.109-131.2004

Free SJ (2013) Fungal cell wall organization and biosynthesis. Adv Genet 81:33–82. https://doi.org/10.1016/B978-0-12-407677-8.00002-6

Galvão MDS, Narain N, Santos MDSPD, Nunes ML (2011) Volatile compounds and descriptive odor attributes in umbu (*Spondias tuberosa*) fruits during maturation. Food Res Int 44(7):1919–1926. https://doi.org/10.1016/j.foodres.2011.01.020

Hammerbacher A, Coutinho TA, Gershenzon J (2019) Roles of plant volatiles in defence against microbial pathogens and microbial exploitation of volatiles. Plant Cell Environ 42(10):2827–2843. https://doi.org/10.1111/pce.13602

Hardin JA, Jones CL, Bonjour EL, Noyes RT, Beeby RL, Eltiste DA, Decker S (2010) Ozone fumigation of stored grain; closed-loop recirculation and the rate of ozone consumption. J Stored Prod Res 46(3):149–154. https://doi.org/10.1016/j.jspr.2010.03.002

Hassanzad Azar H, Taami B, Aminzare M, Daneshamooz S (2018) *Bunium persicum* (Boiss.) B Fedtsch: an overview on phytochemistry, therapeutic uses and its application in the food industry. J Appl Pharm Sci 8(10):150–158. https://doi.org/10.7324/JAPS.2018.81019

Hayaloglu AA, Demir N (2016) Phenolic compounds, volatiles, and sensory characteristics of twelve sweet cherry (*Prunus avium* L.) cultivars grown in Turkey. J Food Sci 81(1):C7–C18. https://doi.org/10.1111/1750-3841.13175

Ho YS, Xiong Y, Ma W, Spector A, Ho DS (2004) Mice lacking catalase develop normally but show differential sensitivity to oxidant tissue injury. J Biol Chem 279(31):32804–32812. https://doi.org/10.1074/jbc.M404800200

Hocking AD, Banks HJ (1991) Effects of phosphine fumigation on survival and growth of storage fungi in wheat. J Stored Prod Res 27(2):115–120. https://doi.org/10.1016/0022-474X(91)90021-4

Hu Z, Yuan K, Zhou Q, Lu C, Du L, Liu F (2021) Mechanism of antifungal activity of *Perilla frutescens* essential oil against *Aspergillus flavus* by transcriptomic analysis. Food Control 123(1):107703. https://doi.org/10.1016/j.foodcont.2020.107703

Jian F, Jayas DS, White NDG (2013) Can ozone be a new control strategy for pests of stored grain? Agric Res 2(1):1–8. https://doi.org/10.1007/s40003-012-0046-2

Johnston LH (1979) The DNA repair capability of *cdc9*, the *Saccharomyces cerevisiae* mutant defective in DNA ligase. Molec Gen Genet 170(1):89–92. https://doi.org/10.1007/BF00268583

Kim D, Langmead B, Salzberg SL (2015) HISAT: a fast spliced aligner with low memory requirements. Nat Methods 12(4):357–360. https://doi.org/10.1038/nmeth.3317

Kong J, Zhang Y, Ju J, Xie Y, Guo Y, Cheng Y, Qian H, Quek SY, Yao W (2019) Antifungal effects of thymol and salicylic acid on cell membrane and mitochondria of *Rhizopus stolonifer* and their application in postharvest preservation of tomatoes. Food Chem 285:380–388. https://doi.org/10.1016/j.foodchem.2019.01.099

Kubo I, Cespedes CL (2013) Antifungal activity of alkanols: inhibition of growth of spoilage yeasts. Phytochem Rev 12(4):961–977. https://doi.org/10.1007/s11101-013-9325-1

Levine B, Kroemer G (2008) Autophagy in the pathogenesis of disease. Cell 132(1):27–42. https://doi.org/10.1016/j.cell.2007.12.018

Li J, Liu J, Zhang H, Xie CH (2011) Identifcation and transcriptional profling of diferentially expressed genes associated with resistance to *Pseudoperonospora cubensis* in cucumber. Plant Cell Rep 30(3):345–357. https://doi.org/10.1007/s00299-010-0959-9

Li S, Zhang S, Zhai H, Lv Y, Hu Y, Cai J (2021) Hexanal induces early apoptosis of *Aspergillus flavus* conidia by disrupting mitochondrial function and expression of key genes. Appl Microbiol Biot 105(18):6871–6886. https://doi.org/10.1007/s00253-021-11543-0

Li Y, Park JS, Deng JH, Bai Y (2006) Cytochrome c oxidase subunit IV is essential for assembly and respiratory function of the enzyme complex. J Bioenerg Biomembr 38(5–6):283–291. https://doi.org/10.1007/s10863-006-9052-z

Li Y, Shao X, Xu J, Wei Y, Wang H (2017a) Effects and possible mechanism of tea tree oil against *Botrytis cinerea* and *Penicillium expansum* in vitro and in vivo test. Can J Microbiol 63(3):219–227. https://doi.org/10.1139/cjm-2016-0553

Li Y, Shao X, Xu J, Wei Y, Xu F, Wang H (2017b) Tea tree oil exhibits antifungal activity against *Botrytis cinerea* by affecting mitochondria. Food Chem 234:62–67. https://doi.org/10.1016/j.foodchem.2017.04.172

Li Z, Shao X, Wei Y, Dai K, Xu J, Xu F, Wang H (2020) Transcriptome analysis of *Botrytis cinerea* in response to tea tree oil and its two characteristic components. Appl Microbiol Biot 104(5):2163–2178. https://doi.org/10.1007/s00253-020-10382-9

Liang D, Xing F, Selvaraj JN, Liu X, Wang L, Hua H, Zhou L, Zhao Y, Wang Y, Liu Y (2015) Inhibitory effect of cinnamaldehyde, citral, and eugenol on aflatoxin biosynthetic gene expression and aflatoxin B_1 biosynthesis in *Aspergillus flavus*. J Food Sci 80(12):M2917–M2924. https://doi.org/10.1111/1750-3841.13144

Livak KJ, Schmittgen TD (2001) Analysis of relative gene expression data using real-time quantitative PCR and the $2^{(-\Delta\Delta CT)}$ Method. Methods 25(4):402–408. https://doi.org/10.1006/meth.2001.1262

Lorini I, Collins PJ, Daglish GJ, Nayak MK, Pavic H (2007) Detection and characterisation of strong resistance to phosphine in Brazilian Rhyzopertha dominica (F.) (Coleoptera: Bostrychidae). Pest Manag Sci 63(4):358–364. https://doi.org/10.1002/ps.1344

Love MI, Huber W, Anders S (2014) Moderated estimation of fold change and dispersion for RNA-seq data with DESeq2. Genome Biol 15(12):550. https://doi.org/10.1186/s13059-014-0550-8

Luo J, Xu F, Zhang X, Shao X, Wei Y, Wang H (2020) Transcriptome analysis of *Penicillium italicum* in response to the flavonoids from *Sedum aizoon* L. World J Microb Biot 36(5):62. https://doi.org/10.1007/s11274-020-02836-z

Lv A, Li C, Tian P, Yuan W, Zhang S, Lv Y, Hu Y (2019) Expression and purification of recombinant puroindoline A protein in *Escherichia coli* and its antifungal effect against *Aspergillus flavus*. Appl Microbiol Biot 103(3):9515–9527. https://doi.org/10.1007/s00253-019-10168-8

Ma W, Zhao L, Xie Y (2017) Inhibitory efect of (*E*)-2-hexenal as a potential natural fumigant on *Aspergillus favus* in stored peanut seeds. Ind Crop Prod 107:206–210. https://doi.org/10.1016/j.indcrop.2017.05.051

Mattiolo E, Licciardello F, Lombardo GM, Muratore G, Anastasi U (2016) Volatile profiling of durum wheat kernels by HS–SPME/GC–MS. Eur Food Res Technol 243(1):147–155. https://doi.org/10.1007/s00217-016-2731-z

Mitchell P (1961) Coupling of phosphorylation to electron and hydrogen transfer by a chemi-osmotic type of mechanism. Nature 191:144–148. https://doi.org/10.1038/191144a0

Papoutsis K, Mathioudakis MM, Hasperué JH, Ziogas V (2019) Non-chemical treatments for preventing the postharvest fungal rotting of citrus caused by *Penicillium digitatum* (green mold) and *Penicillium italicum* (blue mold). Trends Food Sci Tech 86:479–491. https://doi.org/10.1016/j.tifs.2019.02.053

Parveen M, Hasan MK, Takahashi J, Murata Y, Kitagawa E, Kodama O, Iwahashi H (2004) Response of *Saccharomyces cerevisiae* to a monoterpene: evaluation of antifungal potential by DNA microarray analysis. J Antimicrob Chemoth 54(1):46–55. https://doi.org/10.1093/jac/dkh245

Pertea M, Pertea GM, Antonescu CM, Chang TC, Mendell JT, Salzberg SL (2015) StringTie enables improved reconstruction of a transcriptome from RNA-seq reads. Nat Biotechnol 33(3):290–295. https://doi.org/10.1038/nbt.3122

Rocha MEBD, Freire FDCO, Maia FEF, Guedes MIF, Rondina D (2014) Mycotoxins and their effects on human and animal health.

Food Control 36(1):159–165. https://doi.org/10.1016/j.foodcont.2013.08.021

Rutenberg R, Bernstein S, Fallik E, Paster N, Poverenov E (2018) The improvement of propionic acid safety and use during the preservation of stored grains. Crop Prot 110:191–197. https://doi.org/10.1016/j.cropro.2017.09.005

Sharon A, Finkelstein A, Shlezinger N, Hatam I (2009) Fungal apoptosis: function, genes and gene function. FEMS Microbiol Rev 33(5):833–854. https://doi.org/10.1111/j.1574-6976.2009.00180.x

Strzalka W, Ziemienowicz A (2011) Proliferating cell nuclear antigen (PCNA): a key factor in DNA replication and cell cycle regulation. Ann Bot 107(7):1127–1140. https://doi.org/10.1093/aob/mcq243

Suprapta DN, Arai K, Iwai H (1997) Effects of volatile compounds on arthrospore germination and mycelial growth of *Geotrichum candidum* citrus race. Mycoscience 38(1):31–35. https://doi.org/10.1007/BF02464966

Tang X, Shao Y, Tang Y, Zhou W (2018) Antifungal activity of essential oil compounds (geraniol and citral) and inhibitory mechanisms on crain pathogens (*Aspergillus flavus* and *Aspergillus ochraceus*). Molecules 23(9):2108. https://doi.org/10.3390/molecules23092108

Vakifahmetoglu-Norberg H, Ouchida AT, Norberg E (2017) The role of mitochondria in metabolism and cell death. Biochem Bioph Res Co 482(3):426–431. https://doi.org/10.1016/j.bbrc.2016.11.088

Vermes I, Haanen C, Steffens-Nakken H, Reutelingsperger C (1995) A novel assay for apoptosis flow cytometric detection of phosphatidylserine expression on early apoptotic cells using fluorescein labelled Annexin V. J Immunol Methods 184(1):39–51. https://doi.org/10.1016/0022-1759(95)00072-I

Wang N, Shao X, Wei Y, Jiang S, Xu F, Wang H (2021) Quantitative proteomics reveals that tea tree oil effects *Botrytis cinerea* mitochondria function. Pestic Biochem Physiol 164:156–164. https://doi.org/10.1016/j.pestbp.2020.01.005

Wang P, Ma L, Jin J, Zheng M, Pan L, Zhao Y, Sun X, Liu Y, Xing F (2019) The anti-aflatoxigenic mechanism of cinnamaldehyde in *Aspergillus flavus*. Sci Rep 9(1):10499. https://doi.org/10.1038/s41598-019-47003-z

Wang T, Xiu J, Zhang Y, Wu J, Ma X, Wang Y, Guo G, Shang X (2017) Transcriptional responses of *Candida albicans* to antimicrobial peptide MAF-1A. Front Microbiol 8:894. https://doi.org/10.3389/fmicb.2017.00894

Wen P, Chidanguro T, Shi Z, Gu H, Wang N, Wang T, Li Y, Gao J (2018) Identi fi cation of candidate biomarkers and pathways associated with SCLC by bioinformatics analysis. Mol Med Rep 18(2):1538–1550. https://doi.org/10.3892/mmr.2018.9095

Wild CP, Gong YY (2010) Mycotoxins and human disease: a largely ignored global health issue. Carcinogenesis 31(1):71–82. https://doi.org/10.1093/carcin/bgp264

Wu C, Zhang J, Wang M, Du G, Chen J (2012) *Lactobacillus casei* combats acid stress by maintaining cell membrane functionality. J Ind Microbiol Biot 39(7):1031–1039. https://doi.org/10.1007/s10295-012-1104-2

Xu D, Wei M, Peng S, Mo H, Huang L, Yao L, Hu L (2021) Cuminaldehyde in cumin essential oils prevents the growth and aflatoxin B_1 biosynthesis of *Aspergillus flavus* in peanuts. Food Control 125:107985. https://doi.org/10.1016/j.foodcont.2021.107985

Xu J, Shao X, Li Y, Wei Y, Xu F, Wang H (2017) Metabolomic analysis and mode of action of metabolites of tea tree oil involved in the suppression of *Botrytis cinerea*. Front Microbiol 8:1017. https://doi.org/10.3389/fmicb.2017.01017

Xu Y, Wei J, Wei Y, Han P, Dai K, Zou X, Jiang S, Xu F, Wang H, Sun J, Shao X (2020) Tea tree oil controls brown rot in peaches by damaging the cell membrane of *Monilinia fructicola*. Postharvest Biol Tec 175:111474. https://doi.org/10.1016/j.postharvbio.2021.111474

Yu G, Wang L, Han Y, He Q (2012) clusterProfiler: an R package for comparing biological themes among gene clusters. OMICS 16(5):284–287. https://doi.org/10.1089/omi.2011.0118

Zhang S, Qin Y, Li S, Lv Y, Zhai H, Hu Y, Cai J (2021a) Antifungal mechanism of 1-nonanol against *Aspergillus flavus* growth revealed by metabolomic analyses. Appl Microbiol Biot 105(20):7871–7888. https://doi.org/10.1007/s00253-021-11581-8

Zhang W, Lv Y, Lv A, Wei S, Zhang S, Li C, Hu Y (2021b) Sub3 inhibits *Aspergillus flavus* growth by disrupting mitochondrial energy metabolism, and has potential biocontrol during peanut storage. J Sci Food Agric 101:486–496. https://doi.org/10.1002/jsfa.10657

Zhang Y, Damu GLV, Cui S, Mi J, Tangadanchu VKR, Zhou C (2017) Discovery of potential antifungal triazoles: design, synthesis, biological evaluation, and preliminary antifungal mechanism exploration. Medchemcomm 8(8):1631–1639. https://doi.org/10.1039/c7md00112f

Zheng J, Jia Z (2010) Structure of the bifunctional isocitrate dehydrogenase kinase/phosphatase. Nature 465:961–965. https://doi.org/10.1038/nature09088

Zorova LD, Popkov VA, Plotnikov EY, Silachev DN, Pevzner IB, Jankauskas SS, Babenko VA, Zorov SD, Balakireva AV, Juhaszova M, Sollott SJ, Zorov DB (2018) Mitochondrial membrane potential. Anal Biochem 552:50–59. https://doi.org/10.1016/j.ab.2017.07.009